PX-1000: A Solid-State Polarimetric X-Band Weather Radar and Time–Frequency Multiplexed Waveform for Blind Range Mitigation

Boon Leng Cheong, Redmond Kelley, Robert D. Palmer, Yan Zhang, *Member, IEEE*, Mark Yeary, *Senior Member, IEEE*, and Tian-You Yu

***Abstract*— In this paper, a compact, transportable, and dual-polarization X-band weather radar was developed at the Advanced Radar Research Center of the University of Oklahoma. The radar was designed using a software-defined radio (SDR) approach for waveform versatility. One of the key innovations in this paper is the combination of SDR design and the mitigation of blind range, which is inherent in pulse compression radars, using a time–frequency multiplexed waveform while compression is performed in pure software architecture. Internally, this radar has been referred to as the PX-1000. It is primarily used as a platform for waveform studies and various signal processing techniques, such as pulse compression, polarimetric signal processing, refractivity retrieval, and support of various field campaigns. The radar system has been completed and is operational. It has two identical and independent power amplifiers, one for each polarization. The system also features a 1.2-m parabolic reflector dish with dual-polarization feed, which provides a 1.8° beamwidth. A majority of the components are housed above the turntable of an azimuth-over-elevation pedestal. We also took this opportunity to design and develop a new software suite that includes signal processing, system control, and graphical user interface. The raw I/Q time series can be recorded and streamed out of the radar system in real time. In this paper, a detailed description of the radar and some experimental data will be presented.**

***Index Terms*— Chirp modulation, Doppler radar, multiplexing, signal design, signal processing.**

I. Introduction

MANY X-band weather systems have recently gained popularity as they are relatively smaller in size, lightweight, transportable, and work well for short range data collections [1]–[3]. Examples of such systems include the CASA IP-1 network [3], X-Pol from the University of Massachusetts-Amherst (UMass) [4], NO-XP from the National Severe Storms Laboratory [5], and Doppler on Wheels (DOW) and Rapid DOW from the Center for Weather Research [6], [7], just to name a few. As the operating wavelength becomes shorter, compared with wavelengths in the S and C bands, smaller particles can be detected [8] providing additional details on the microphysics of storms.

For close range, a radar can still produce high spatial resolution observations even at a 2°-beamwidth, which is important for rapidly evolving events, such as tornado genesis [9]. Such applications have been accomplished, for example, using the UMass X-Pol and the MWR-05XP from the Center for Interdisciplinary Remotely-Piloted Aircraft Studies [10]. Funded by the National Science Foundation, a mobile X-band radar that is capable of performing a complete sweep in just 2 s has recently been developed by the Pro-Sensing, which has been referred to as the Rapid X-band Polarimetric radar [11], [12].

Because of their transportability, mobile weather radars have been used in a number of occasions for storm capture field campaigns. The largest campaign to date is the Verification of the Origins of Rotation in Tornadoes Experiment, Part 2, where 10 mobile radars were deployed to capture radar data of tornado events [5], [13]–[15]. As the project name suggests, the primary objective was to understand tornadoes. Mobile radars are a good choice as they can be quickly relocated to areas where the tornadoes are most likely to occur. Mobile facilities can also be used to reach out to people who may not have access to radars for educations, such as the Shared Mobile Atmospheric Radar for Teaching and Research [16].

Of course, X-band weather radars have several challenges. One of them is the significant attenuation effects through storms, which is problematic for quantitative precipitation estimation [17]. While reflectivity calibration has always been a challenge for weather radars [18], recent work in polarimetry has shown significant promise to mitigate attenuation correction [19]–[22].

Most existing X-band weather radars are magnetron-based in which techniques such as phase coding for range unfolding and pulse compression are not possible. In this project, a solid-state, software-defined, configurable coherent radar system is developed at the Advanced Radar Research Center (ARRC) of the University of Oklahoma (OU). Internally, this radar has

Manuscript received December 3, 2012; revised February 8, 2013; accepted March 4, 2013. Date of publication July 15, 2013; date of current version October 7, 2013. This work was supported by the State of Oklahoma and Regents for Higher Education under Project 091007. The Associate Editor coordinating the review process was Dr. Matteo Pastorino.

B. L. Cheong and R. Kelley are with the Advanced Radar Research Center, University of Oklahoma, Norman, OK 73072 USA (e-mail: boonleng@ou.edu; redmond@ou.edu).

R. D. Palmer is with the Advanced Radar Research Center, University of Oklahoma, Norman, OK 73072 USA, and also with the School of Meteorology, University of Oklahoma, OK 73072 USA (e-mail: rpalmer@ou.edu).

Y. Zhang, M. Yeary, and T.-Y. Yu are with the Advanced Radar Research Center, University of Oklahoma, Norman, OK 73072 USA, and also with the School of Electrical and Computer Engineering, University of Oklahoma, OK 73072 USA (e-mail: rockee@ou.edu; yeary@ou.edu; tyu@ou.edu).

Color versions of one or more of the figures in this paper are available online at http://ieeexplore.ieee.org.

Digital Object Identifier 10.1109/TIM.2013.2270046

been referred to as the PX-1000. The key idea was conceived in the year of 2008, in which the last two digits 08 in binary are represented as 1000. We envisioned the radar to be used as a testbed for waveform studies as well as various signal processing techniques, such as pulse compression, polarimetric signal processing, refractivity retrieval, and supplemental validation for experiment campaigns. The concept of pulse compression radar is not new at all. Numerous concepts and demonstrations have been presented in the literature, (See [23]-–[27]), but its application to weather observation is still limited [28] and that was one of the primary motivations for this paper.

The PX-1000 system has been completed and has been operational since mid-2012. Some data will be presented in this paper. As mentioned in the abstract, the radar is designed using a software-defined radio approach for system versatility, where many of the analog components such as mixers, filters, and modulators are implemented in the digital transceiver system as software [29]–[32]. One of the key differences between this system and other X-band systems is the dual-channel digital transceiver integrated in the radar system with independent transmit and receive chains, i.e., independent up-down converters and power amplifiers.

The rest of this paper is organized as follows. First, the waveform versatility of the PX-1000 and the time–frequency multiplexed (TFM) waveform for blind range mitigation will be discussed in Section II. Then, an overview of system hardwave and software will be presented in Section III. Experimental results will be delivered in Section IV and finally our future work will be presented in Section V.

II. Waveform Versatility

A software-defined radar with a digital transceiver and solid-state amplifiers provides the versatility of using arbitrary waveforms. While Klystron amplifiers also provide this flexibility, they are generally more expensive. Solid-state and Traveling Wave Tube, amplifiers both offer the same phase coherency feature with peak powers that are lower than Klystrons with solid-state power amplifiers available at lower costs [33]. Due to the low peak power output, the average power is compensated by transmitting longer pulses, which reduces the range resolution that is directly proportional to the pulse width. It can, however, be recovered by using pulse compression techniques [23], [28], [34]. One unique feature of the PX-1000 is the twin independent transmit-receive chains, i.e., the transmit waveforms for each channel can be different so that various waveform configurations can be explored. For example, one could potentially use a pair of waveforms (or codes) that simultaneously achieve pulse compression and cross-channel isolation enhancement [35], or a pair of waveforms that equalize the channel response of the system independently. With a digital transceiver, arbitrary digital samples can be used in the digital-to-analog conversion to accomplish any desired waveforms at intermediate frequencies (IF), such as subpulse phase-coded waveforms, interpulse phase-coded waveforms, and frequency-coded waveforms.

A. TFM Waveform

As mentioned earlier, to compensate the relatively low peak power output of the transmitters, long pulse widths are used to regain the radar sensitivity. Two major disadvantages of doing so are the loss of range resolution and the blind range. Even if the system is capable of sampling the signals during the transmit duty cycle, the leak through transmit signal from the circulator generally overwhelms the return signals and causes the near-range signals to be unusable and, thus, the radar is considered to be blind during that time. One mitigation strategy involves interleaving a set of short and long pulses at the pulse repetition time (PRT) interval, resulting in a waveform switching transmission. An apparent disadvantage of doing so is the loss of maximum unambiguous velocity as the effective PRT for each waveform is increased by a factor of two.

In this paper, we developed a TFM waveform to simultaneously accomplish pulse compression and mitigate the blind range limitation. The key is to use a set of two waveforms that are separated in frequency but multiplex them in time to create a single pulse. That is, the waveform generator (of the transceiver) considers the entire TFM waveform as one pulse. The order of the subwaveform must be arranged from the longest to the shortest since the entire transmit cycle is considered to be blind. With the short pulse at the end, one can think of it as another radar operating at a slightly different frequency at a synchronized but delayed pulsing scheme. As such, the blind range is now just the duration of the short pulse, which is negligible, i.e., on the orders of tens of meters. A similar approach has been proposed by [36] using frequency diversified waveform and simulated results using radar moment data were presented. Fig. 1 shows the instantaneous frequency function and the multiplexing scheme of the waveform. One can think of it as a time concatenation of two waveforms that occupy different frequency bands. In this paper, the optimization of each waveform is not considered but it is one of the current research topics and will be presented in a separate study. Similar to a conventional rectangular pulse, the waveform generator produces a complete TFM waveform when it receives a trigger signal. This method is different from the waveform interleaving method, i.e., TFM waveform does not suffer the loss of effective PRT. In fact, staggered PRT method can be implemented more easily using the TFM waveform compared with the interleaving method. In addition, TFM can be expanded to be a multiplex of three or four waveforms. The expansion is straightforward and for the sake of simplicity, the following discussion focuses on a two-waveform configuration. Fig. 2 shows a measured waveform and its performance through the radar system.

At the receiver, the waveform is decoded into two parts. The fundamental idea is to apply match filtering twice to the time series. One uses the long waveform, while the other uses the short waveform as the matched filter. The pulse compression algorithm is implemented in the Fourier domain for computational efficiency by exploiting the mathematical property that a matched filtering is essentially a convolution in the time domain of the input signal $x[n]$ with a time-reversed

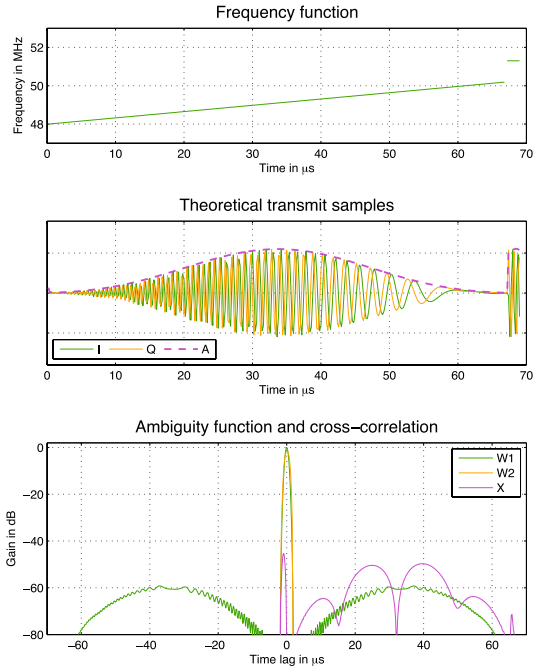

Fig. 1. Frequency function of the TFM waveform (top) and its theoretical baseband I/Q samples (middle). The compressed response represents the auto-correlation of each subwaveform, denoted W1 for the long waveform, W2 for the short waveform, and X for their cross-correlation (bottom).

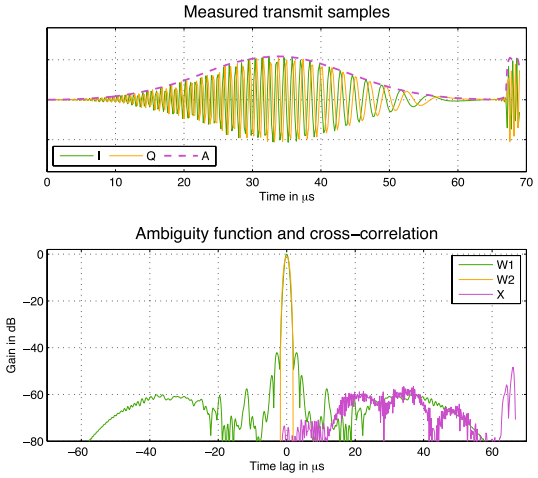

Fig. 2. Measured TFM waveform through the coupler at the transmitter (top) and its performance (bottom).

complex conjugate of the transmit waveform $t[n]$, denoted as $t^*[-n]$, which is equivalent to a multiplication of their counterparts in the Fourier domain. The compressed signal $y[n]$ is obtained by applying the inverse Fourier transform to the result of the multiplication. This technique is fairly common in High-Performance Embedded Computing for signal filtering using long filters [37]. Mathematically, it can be described as follows:

$$y[n] = x[n] * t^*[-n] \leftrightarrow \mathrm{X}(j\omega)\mathrm{T}(-j\omega) \quad (1)$$

$$\leftrightarrow \mathrm{X}(j\omega)\mathrm{T}^*(j\omega) \quad (2)$$

where $X(j\omega)$ and $T(j\omega)$ represent the Fourier transform of the input signal and waveform signal, respectively. In the PX-1000 radar, the waveform signal is obtained from a coupler

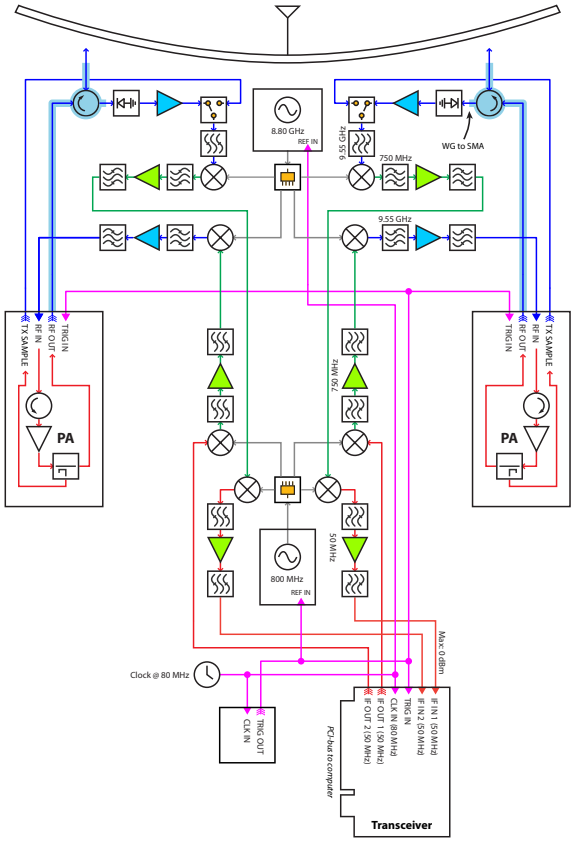

Fig. 3. System block diagram of the PX-1000. Each polarization channel is independent of each other allowing distinct waveforms to be used.

in between the transmitter and circulator. A fast switch is used to route the transmit signal through the receive path to provide a sample of the transmit waveform, then immediately switch to receive from the antenna at each pulse. For the TFM waveform with two subwaveforms $w_1[n]$ and $w_2[n]$, the process in (2) is repeated for each subwaveform and their corresponding compressed signals are combined to produce the final compressed signal $y[n]$, which is subsequently used for radar product calculations. Note from (2) that the template need not be time-reversed, a complex conjugate operator (negate the imaginary component) can be used to reduce the amount of computations. The complete process of matched filtering and waveform demultiplexing is summarized as follows.

1) Compute the zero-padded fast Fourier transform (FFT) of the data, $\mathrm{X}(j\omega)$, and the filters, $\mathrm{W}_1(j\omega)$ and $\mathrm{W}_2(j\omega)$.
2) Compute $\mathrm{Y}_1(j\omega)$, the product of $\mathrm{X}(j\omega)$ and $\mathrm{W}_1{}^*(j\omega)$.
3) Compute $y_1[n]$, the inverse Fourier transform of $\mathrm{Y}_1(j\omega)$.
4) Compute $\mathrm{Y}_2(j\omega)$, the product of $\mathrm{X}(j\omega)$ and $\mathrm{W}_2{}^*(j\omega)$.
5) Compute $y_2[n]$, the inverse Fourier transform of $\mathrm{Y}_2(j\omega)$.
6) Generate $y[n]$ by choosing in between $y_1[n]$ and $y_2[n]$ for the appropriate range gates.

B. Computation Efficiency

The overhead to implement the matched filtering process in the Fourier domain is, of course, the Fourier transforms. Such processing is only worthwhile when the filter length is long, which is precisely the case here for pulse compression.

Fig. 4. Photographs of the finished system (top) and the fully assembled trailer in a field experiment (bottom).

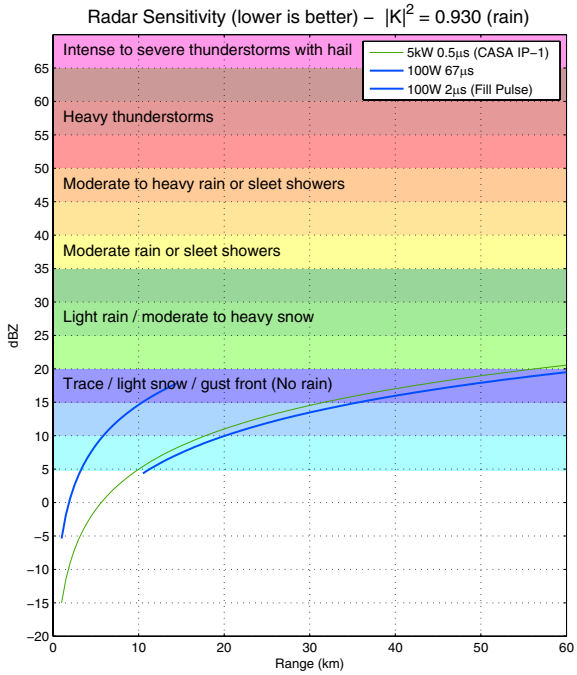

Fig. 5. Radar sensitivity of the PX-1000. The radar is suitable for precipitation measurements, i.e., reflectivity of 20 dBZ and above.

TABLE I
SYSTEM CHARACTERISTICS OF THE PX-1000

General	
Operating frequency	9550 MHz
Typical PRF	2000 Hz
Typical observation range	60 km
Antenna (Seavey Antenna C0824-820)	
Antenna gain	38.5 dBi
Diameter	1.2 m
3-dB beamwidth	1.8°
Polarimetric isolation	26 dB
Polarization	dual linear
Pedestal (Orbit Technology Group AL-4016)	
Elevation coverage	-2° to 182°
Maximum payload	120 kg
Maximum angular velocity	50° s^{-1}
Pointing precision	0.25°
Angular feedback precision	16 bit
Solid-state Transmitters (In-house assembly)	
Peak power	100 W
Maximum pulse width	69 μs
Typical / maximum duty cycle	14% / 20%
IF Transceiver (Pentek 7140)	
IF frequency	50 MHz
Analog-to-digital quantization	14 bit
Receive bandwidth	5 MHz
Typical gate spacing	30 m
Maximum data throughput	320 Mbps

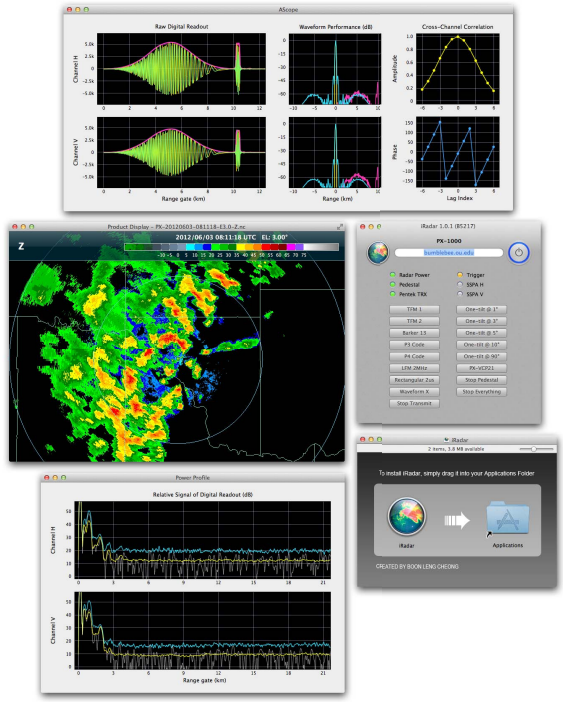

Fig. 6. Here are some screenshots of the radar GUI. Top window is the AScope display, middle left window is a product display, middle right window is the main control interface, bottom left window is a power profile display, and bottom right is a screenshot of installation procedure.

Otherwise, a cross-correlation function would be a more straightforward implementation. For the PX-1000, the raw data are processed on a conventional PC with an x86 CPU (e.g., Intel Core i5 2.4 GHz) using the FFTW3 library [38]. To show the computational requirements of these two methods, consider this example: a pulse that is collected with 2000 gates and a filter length of 350 samples. For a radar gate spacing of 30 m, they correspond to 60 km range and 10.5 km pulse width, which are typical parameters for the PX-1000 during operations. We will use the number of floating point operation (FLOP) to quantitatively illustrate the point.

Each complex multiply consumes six FLOPs. One can readily see that the cross-correlation method would require 700 000 (350 samples for each range gate for 2000 gates) complex

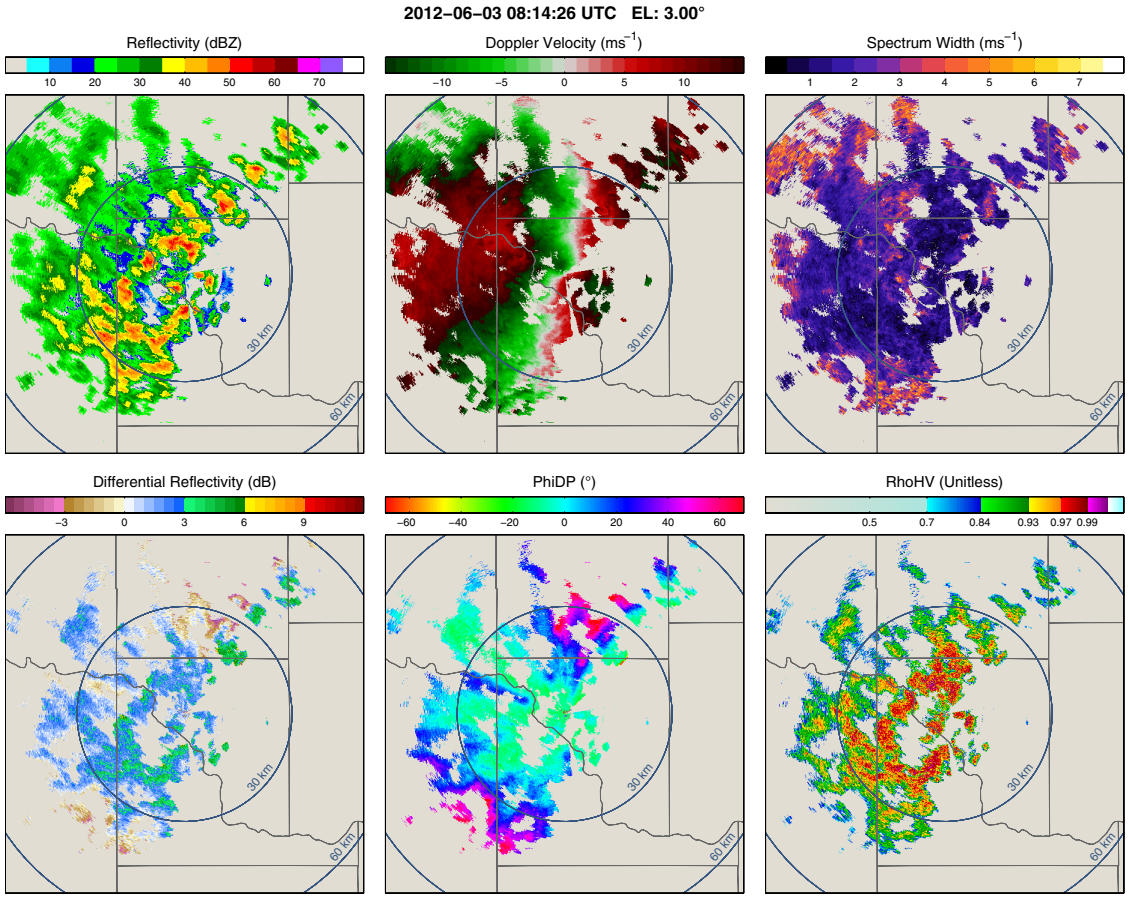

Fig. 7. Base moment data and polarimetric variables collected using the PX-1000 on 2012-06-03 08:20 UTC. From left to right, the top panels show reflectivity, Doppler velocity and spectrum width, the bottom panels show differential reflectivity, differential phase and correlation coefficient.

multiplications (six FLOPs) and 700 000 complex additions (two FLOPs), which summed up to be 56 MegaFLOPs per pulse. If the radar is operating at pulse repetition frequency (PRF) of 1000 Hz, the computational requirement would be 56 GigaFLOP (GFLOPS)/s, which is a demanding requirement even for modern CPUs. The actual computation requirements would also need to factor in overhead for data transports and loop counting but in the realm of this discussion, we will neglect this overhead as it is similar for both methods. For the Fourier domain implementation, the computational costs of the FFT would need to be considered for a fair comparison. In practice, a radix-2, zero-padded, N-length complex FFT requires approximately $5N\log(N)$ FLOPS [39]. For $N = 2048$, that is 112 640 FLOPs. The whole process of filtering requires three FFT operations, i.e., one for the pulse data, one for the waveform template, and one for the inverse of the result. Together with N complex multiplications and additions in the Fourier domain, the whole process consumes 354 304 FLOPs. At the same PRF, it requires only 0.35 GFLOPS, which is only a small fraction of the computation requirement for the cross-correlation method.

III. Hardware and Software

A system block diagram of the PX-1000 is depicted in Fig. 3. The operating frequency of the radar is selected to be at 9550 MHz as a result of using the IF at 50 MHz and a two-stage up–down conversion (UDC) process with local oscillator (LO) frequencies at 800 MHz and 8800 MHz. These LO frequencies are integer multiples of the 80 MHz reference signal. Using this two-stage UDC architecture, we can eliminate the need for extremely narrow-band bandpass filters at X-band, which is difficult to fabricate. A majority of the analog signal components, transceiver, and main host for the signal processing are housed above the turntable of the pedestal, immediately behind the dish. An in-house trigger generator assembly was designed and developed, which produces a set of synchronized trigger signals that are used throughout the system. Fig. 4 shows a picture of the complete radar and the entire trailer unit during a field experiment. Within the housing at each arm of the pedestal, there is a Rack Unit enclosure housing the UDC systems. One of the UDC boxes houses the master oscillator where the 80-MHz reference signal is generated. The reference signal is distributed throughout the system. The system characteristics of the PX-1000 are summarized in Table I.

With a 100-W transmitter and TFM waveform described in Section II-A, the radar sensitivity of up to 60-km range can be derived mathematically using the radar equation and is shown in Fig. 5. At this sensitivity, the radar is capable of capturing most echoes from typical precipitations, i.e., 20 dBZ and above.

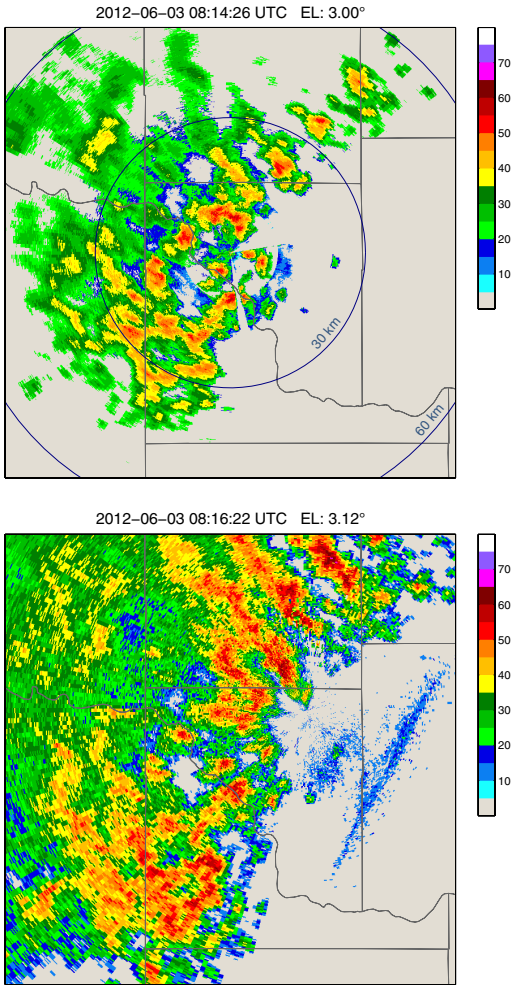

Fig. 8. Reflectivity maps from the PX-1000 (top) and the KTLX (bottom), an operational WSR-88D radar. Signal attenuation through rain in the data from the PX-1000 is evident but in the scope of this paper, the rain attenuation is not corrected. Most moderate to heavy rainfall signals are all captured within 60 km. Signal extinctions are as expected through heavy rainfall.

Software development is also another major effort in this paper. We took the opportunity to design and develop a new suite of software for data acquisition, signal processing, system controls, communication, and user interface. With the complete ownership of the software sources, various levels of the software architecture is directly accessible, which provides us the absolute freedom to modify and engineer the system. Take the time-series filtering and demultiplexing of the TFM waveform for example, it is only possible with complete access to the raw data and the data feeding mechanism during the demultiplexing process. That is, the raw data have to be ingested to the pulse-compression module and the compressed pulse needs to be fed to the subsequent radar product generator with minimal overhead, as this process is repeated at every pulse. Other than the hardware-related components, the signal processing portion of the software was developed with no propriety framework dependency for portability. It is coded in plain C language, which can be easily migrated and applied to various operating systems.

The transceiver and pedestal components of the software rely on their vendors' Application Programming Interface for hardware interactions. They are, however, developed to be standalone and are loosely coupled with the rest of the software components. That is, only high-level message exchange for instructions and feedback keep them connected, if needed. Otherwise, they would function as standalone applications. At the transceiver, once the angular reading and time-series are combined, the radar data transmission is accomplished with our newly developed framework that can be applied to other systems, with moderate engineering, to facilitate tasks such as offline data playback or time-series data ingest from another radar.

A suite of software for the graphical user interface (GUI) to control the radar was also developed. We chose to develop Mac OS X for the ease of installation, in which most Mac users would be familiar with, i.e., a drag-and-drop process. Internally, we referred it as the iRadar. Fig. 6 shows example screenshots of iRadar including the main control interface, A-scope and product viewer for live view of the datastream and offline product inspections.

IV. Experimental Results

Using the TFM waveform described in Section II, a data set was collected on 2012-06-03 08:20 UTC when an event of isolated storm cells approached Norman, Oklahoma. The transmit waveform was setup to use a total of 69-μs pulse width, with the long waveform occupying 67 μs and the fill pulse occupying 2 μs. Fig. 7 shows a snapshot of the data set. There are six panels in the figure, showing reflectivity in dBZ, Doppler velocity in ms^{-1}, spectrum width in ms^{-1}, differential reflectivity in dB, differential phase (ϕ_{DP}) in degrees (°), and normalized cross-pol coefficient (ρ_{HV}). One can readily see that there is no blind range in the data set. Besides filling the blind range, using TFM waveform suffers no penalty in the effective PRF. In this case, with a 2000 Hz PRF, the aliasing velocity is 15 ms^{-1}.

In general, all the base data and polarimetric variables appear normal with the pulse compression technique as expected, the radar suffers signal attenuation through rain because of the radar wavelength in X-band. It can be seen from the data that differential reflectivity and ϕ_{DP} exhibit signatures of attenuation, which can be used for correction using several existing techniques [21], [40]–[43]. Ignoring the signal attenuation issue for the sake of validating the working conditions of the radar, a snapshot of the reflectivity map from a nearby operational WSR-88D radar, the KTLX, is shown in Fig. 8 for comparison. One can see that the radar captures most returns from moderate to heavy rainfall except regions where signal extinction occurs through heavy rainfall, i.e., outer range of the domain, especially in the northern and south-western regions.

Fig. 9 shows a close-up view near the transition range at approximately 10 km, annotated by the dashed-line ring. Without the use of the TFM waveform, data in this range would not be available. For short-range radars that are targeted to cover 40–60 km range, this represents a significant blind range if no mitigation procedure is done. As mentioned earlier, a simple remedy would be to use an interleaving pulse scheme

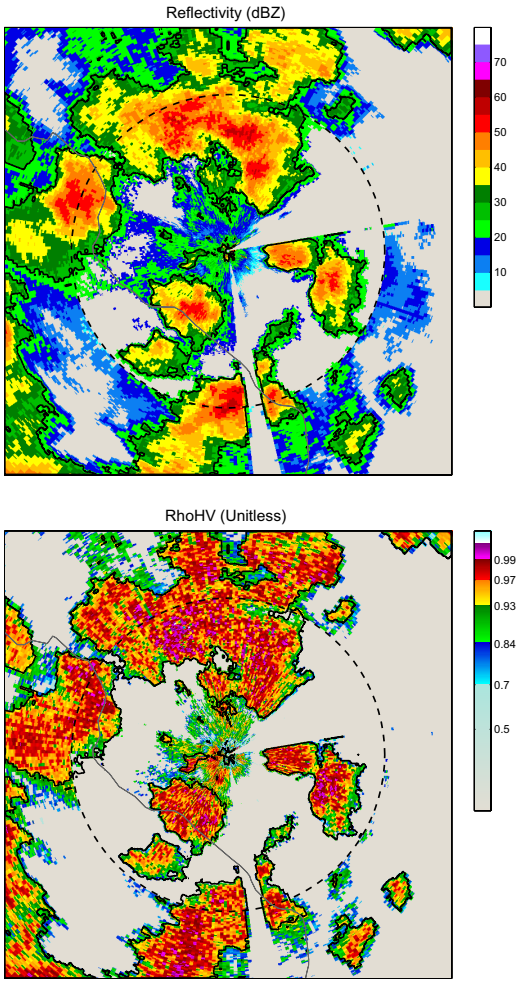

Fig. 9. Close-up view of reflectivity (top) and correlation coefficient (bottom) near the transition range at approximately 10 km. Sensitivity gain from the short pulse to long pulse is as expected. Without the use of a fill pulse in TFM, data within this range would not be available. Contour line is shown moderate to heavy rainfall ($Z \geq 25$ dBZ) and it can be seen that transition from short to long waveform in this region is smooth and seamless.

that alternate between short and long pulses to scan for the short and long ranges but the TFM waveform can also be used to rectify this situation. The advantage of the later is that there is no loss of effective PRF for each waveform, which maintains the aliasing velocity. This is especially important for X-band radars as Doppler velocity fields are commonly aliased. Unfolding the velocity field can still be accomplished but would become even more challenging for a multiple-time aliased field.

By inspecting reflectivity data near the transition range, one can observe the sensitivity gain from short waveform to long waveform. The transition in the merged data derived from the two demultiplexed waveform is evident, shown by the blue shades (reflectivity in between 10 and 20 dBZ) which is an indication that the long waveform is sufficiently sensitive to detect drizzle and very light rain. While the reflectivity factor can be calibrated to have reflectivity values derived from both waveforms match, the underlying signal-to-noise ratio is actually very low for the short waveform, near the transition range. The effect is manifested into lower ρ_{HV} values, as seen in the second panel of Fig. 9. One way around this is by using a TFM waveform that is a multiplex of more subwaveforms to obtain a more subtle transition. This would require wider hardware bandwidth, which is currently not available with the PX-1000 but this result has demonstrated the ability to recover blind range using a TFM waveform for transmit and a demultiplexing mechanism.

In addition to ρ_{HV}, Z_{DR}, and ϕ_{DP} also exhibit discontinuities in the transition range. We are convinced that all moment data inherit some degrees of bias. An obvious culprit would be the integration effects through the sidelobes, which can be seen from the compressed response of the waveform. Note the asymmetrical interference levels between the long and short subwaveform in Fig. 1 at different ranges. Such inteference means a bias from the other subwaveform is introduced, which is also a function of the signal strength at different range where the sidelobes reside. Therefore, a low integrated sidelobe level is desired.

V. Conclusion

With a flexible waveform generator in the PX-1000, there is a parallel effort at OU-ARRC to investigate and develop minimally-tapered waveforms for pulse compression. The main goal is to maximize the radar sensitivity and power efficiency using an optimization algorithm. In addition, we will also investigate various waveform designs for pulse compression and waveform-coding techniques to seek the possibilities of improving the system performance.

Recent signal processing techniques such as multilag signal processing for enhancing polarimetric measurements [44], radar refractivity retrieval [45], [46], and ground clutter filtering will be incorporated into the system in the near future.

We are also currently investigating the possibility of integrating PX-1000 into CASA network [3] in Dallas–Fort Worth for field campaigns given that PX-1000 and the CASA radars share many system specifications.

Acknowledgment

The authors would like to thank S. Frasier, D. McLaughlin, M. Zink, and E. Knapp from the University of Massachusetts, MA, USA, for their help and insights, and would also like to thank C. Koehler, J. Meier, I. Meier, B. Isom, and D. Bodine from the ARRC for all their help, comments, ideas, and suggestions.

References

[1] S. Y. Matrosov, D. E. Kingsnill, and F. M. Ralph, "The utility of X-band polarimetric radar for quantitative estimates of rainfall parameters," *J. Hydrometeorol.*, vol. 6, no. 3, pp. 248–262, 2005.

[2] J. A. Brotzge, K. K. Droegemeier, and D. J. McLaughlin, "Collaborative Adaptive Sensing of the Atmosphere (CASA): New radar system for improving analysis and forecasting of surface weather conditions," *J. Transp. Res. Board*, vol. 1948, pp. 145–151, Dec. 2006.

[3] D. McLaughlin, D. Pepyne, B. Philips, J. Kurose, M. Zink, D. Westbrook, E. Lyons, E. Knapp, A. Hopf, A. Defonzo, R. Contreras, T. Djaferis, E. Insanic, S. Frasier, V. Chandrasekar, F. Junyent, N. Bharadwaj, Y. Wang, Y. Liu, B. Dolan, K. Droegemeier, J. Brotzge, M. Xue, K. Kloesel, K. Brewster, F. Carr, S. Cruz-Pol, K. Hondl, and P. Kollias, "Short-wavelength technology and the potential for distributed networks of small radar systems," *Bull. Amer. Meteorol. Soc.*, vol. 90, no. 12, pp. 1797–1817, Dec. 2009.

[4] F. Junyent, A. Pazmany, H. Bluestein, M. R. Kramar, M. French, C. Weiss, and S. Frasier, "Dual-polarization, mobile, X-band, Doppler-radar observations of hook echoes in supercells," in *Proc. 22nd Conf. Severe Local Storms*, Oct. 2004, pp. 1–13, p. P11.7.

[5] C. M. Schwarz and D. W. Burgess, "Verification of the origin of rotation in tornadoes experiment, Part 2 (VORTEX2): Data from the NOAA (NSSL) X-band dual-polarized radar," in *Proc. 25th Conf. Severe Local Storms*, Oct. 2010, pp. 1–16, p. P6.1.

[6] J. Wurman, J. Straka, E. Rasmussen, M. Randall, and A. Zahrai, "Design and development of a portable, pencil-beam, pulsed, 3-cm Doppler radar," *J. Atmos. Ocean. Technol.*, vol. 14, no. 12, pp. 1502–1512, 1997.

[7] J. Wurman and M. Randall, "An inexpensive, mobile, rapid-scan radar," in *Proc. 30th Conf. Radar Meteorol.*, 2001, pp. 1–3, pp. CD–ROM P3.4.

[8] R. Lhermitte, "A 94 GHz Doppler radar for clouds observations," *J. Atmos. Ocean. Technol.*, vol. 4, pp. 36–48, Mar. 1987.

[9] H. Bluestein, M. M. French, R. L. Tanamachi, S. Frasier, K. Hardwick, F. Junyent, and A. Pazmany, "Close-range observations of tornadoes in supercells made with a dual-polarization, X-band, mobile Doppler radar," *Monthly Weather Rev.*, vol. 135, no. 4, pp. 1522–1543, 2007.

[10] H. Bluestein, M. M. French, I. PopStefanija, R. T. Bluth, and J. B. Knorr, "A mobile, phased-array Doppler radar for the study of severe convective storms: The MWR-05XP," *Bull. Amer. Meteorol. Soc.*, vol. 91, no. 5, pp. 579–600, 2010.

[11] A. Pazmany and H. Bluestein, "Mobile rapid scanning X-band polarimetric (RaXpol) Doppler radar system," in *Proc. 34th Conf. Radar Meteorol.*, Oct. 2009, pp. 1–6, p. 8A.2.

[12] A. Pazmany and H. Bluestein, "Mobile rapid scanning X-band polarimetric (RaXpol) Doppler radar system," in *Proc. 35th Conf. Radar Meteorol.*, 2011, pp. 1–3, p. 16B.2.

[13] D. W. Burgess, E. R. Mansell, C. M. Schwarz, and B. J. Allen, "Tornado and tornadogenesis events seen by the NOXP, x-band, dual-polarization radar during VORTEX2 2010," in *Proc. Preprints, 25th Conf. Severe Local Storms*, Oct. 2010, pp. 1–17, p. 5.2.

[14] H. B. Bluestein, M. M. French, J. B. Houser, J. C. Snyder, R. L. Tanamachi, I. PopStefanija, C. Baldi, G. D. Emmitt, V. Venkatesh, K. Orzel, S. J. Frasier, and R. T. Bluth, "A summary of data collected during VORTEX2 by MWR-05XP/TWOLF, UMass X-Pol, and the UMass W-band radar," in *Proc. Preprints, 25th Conf. Severe Local Storms*, Oct. 2010, pp. 1–5, p. 5.4.

[15] J. Wurman, L. Wicker, Y. Richardson, P. Markowski, D. Dowell, D. Burgess, and H. Bluestein, "Vortex2: The verification of the origins of rotation in tornadoes experiment," in *Proc. Preprints, 25th Conf. Severe Local Storms*, Oct. 2010, pp. 1–10, p. 5.1.

[16] M. Biggerstaff, L. Wicker, J. Guynes, C. Ziegler, J. Straka, E. Rasmussen, I. A. Doggett, L. Carey, J. Schroeder, and C. Weiss, "The shared mobile atmospheric research and teaching radar: A collaboration to enhance research and teaching," *Bull. Amer. Meteor. Soc.*, vol. 86, no. 9, pp. 1263–1274, 2005.

[17] A. V. Ryzhkov and D. S. Zrnić, "Comparison of dual-polarization radar estimators of rain," *J. Atmos. Ocean. Technol.*, vol. 12, no. 2, pp. 249–256, Apr. 1995.

[18] D. Atlas, "Radar calibration: Some simple approaches," *Bull. Amer. Meteor. Soc.*, vol. 83, no. 9, pp. 1313–1316, 2002.

[19] S. Y. Matrosov, K. A. Clark, B. E. Martner, and A. Tokay, "X-band polarimetric radar measurements of rainfall," *J. Appl. Meteorol.*, vol. 41, pp. 941–952, Sep. 2002.

[20] A. Illingworth and T. Blackman, "The need to represent raindrop size spectra as normalized Gamma distributions for the interpretation of polarization radar observations," *J. Appl. Meteorol.*, vol. 41, no. 3, pp. 286–297, 2002.

[21] J. Vivekanandan, G. Zhang, S. Ellis, D. Rojapadhyaya, and S. Avery, "Radar reflectivity calibration using differential propagation phase measurement," *Radio Sci.*, vol. 38, no. 3, pp. 1–14, 2003.

[22] A. V. Ryzhkov, S. E. Giagrande, V. M. Melnikov, and T. Schuur, "Calibration issues of dual-polarization radar measurements," *J. Atmos. Ocean. Technol.*, vol. 22, pp. 1138–1155, Aug. 2005.

[23] J. R. Klauder, A. C. Price, S. Darlington, and W. J. Albersheim, "The theory and design of chirp radars," *Bell Syst. Tech. J.*, vol. 39, no. 4, pp. 745–808, Jul. 1960.

[24] B. L. Lewis and F. F. Kretchmer, "Linear frequency modulation derived polyphase pulse compression codes," *IEEE Trans. Aerosp. Electron. Syst.*, vol. 18, no. 5, pp. 637–641, Sep. 1982.

[25] K. M. El-Shennawy, O. A. Alim, and M. A. Ezz-El-Arab, "Linear FM chirp filters in pulse compression radars," *IEEE Trans. Instrum. Meas.*, vol. 36, no. 3, pp. 783–788, Sep. 1987.

[26] K. Nakahira, T. Kodama, T. Furuhashi, and H. Maeda, "Design of digital polarity correlators in a multiple-user sonar ranging system," *IEEE Trans. Instrum. Meas.*, vol. 54, no. 1, pp. 305–310, Feb. 2005.

[27] S. Kurokawa, M. Hirose, and K. Komiyama, "Measurement and uncertainty analysis of free-space antenna factors of a log-periodic antenna using time-domain techniques," *IEEE Trans. Instrum. Meas.*, vol. 58, no. 4, pp. 1120–1125, Apr. 2009.

[28] V. Chandrasekar and R. J. Keeler, "Pulse compression for weather radars," *IEEE Trans. Geosci. Remote Sens.*, vol. 36, no. 1, pp. 125–142, Jan. 1998.

[29] M. Dillinger, K. Madani, and N. Alonistioti, *Software Defined Radio: Architectures, Systems and Fucntions*. New York, NY, USA: Wiley, 2003.

[30] F. Harris and R. W. Lowdermilk, "Software defined radio: Part 22 in a series of tutorials on instrumentation and measurement," *IEEE Instrum. Meas. Mag.*, vol. 13, no. 1, pp. 23–32, Feb. 2010.

[31] J. Meier, R. Kelley, B. Isom, M. Yeary, and R. Palmer, "Leveraging software-defined radio techniques in multichannel digital weather radar receiver design," *IEEE Trans. Instrum. Meas.*, vol. 61, no. 6, pp. 1571–1582, Jun. 2012.

[32] M. Yeary, G. Crain, A. Zahrai, C. Curtis, J. Meier, R. Kelley, I. Ivic, R. D. Palmer, R. J. Doviak, G. Zhang, and T.-Y. Yu, "Multichannel receiver design, instrumentation, and first results at the national weather radar testbed," *IEEE Trans. Instrum. Meas.*, vol. 61, no. 7, pp. 2022–2033, Jul. 2012.

[33] A. Duzdar and G. Kompa, "Applications using a low-cost baseband pulsed microwave radar sensor," in *Proc. IEEE Trans. Instrum. Meas. Conf.*, May 2001, pp. 239–243.

[34] R. B. Rybdal, K. H. Hurlbut, and T. T. Mori, "High-resolution instrumentation radar," *IEEE Trans. Instrum. Meas.*, vol. 36, no. 1, pp. 110–114, Mar. 1987.

[35] V. Chandrasekar and N. Bharadwaj, "Orthogonal channel coding for simultaneous co- and cross-polarization measurements," *J. Atmos. Ocean. Technol.*, vol. 26, pp. 45–56, Jan. 2009.

[36] N. Bharadwaj and V. Chandrasekar, "Wideband waveform design principles for solid-state weather radars," *J. Atmos. Ocean. Technol.*, vol. 29, pp. 14–31, Jan. 2012.

[37] D. R. Martinez, R. A. Bond, and M. M. Vai, *High Performance Embedded Computing Handbook: A System Perspective*. Cleveland, OH, USA: CRC Press, 2008.

[38] M. Frigo and S. G. Johnson, "The design and implementation of FFTW3," *Proc. IEEE*, vol. 93, no. 2, pp. 216–231, Feb. 2005.

[39] J. W. Cooley and J. W. Tukey, "An algorithm for the machine computation of the complex Fourier series," *Math. Comput.*, vol. 19, pp. 297–301, Apr. 1965.

[40] V. N. Bringi and V. Chandrasekar, *Polarimetric Doppler Weather Radar: Principles and Applications*. Cambridge, U.K.: Cambridge Univ. Press, 2001.

[41] E. Gorgucci and V. Chandrasekar, "Evaluation of attenuation correction methodology for dual-polarization radars: Application to X-band systems," *J. Atmos. Ocean. Technol.*, vol. 22, no. 8, pp. 1195–1206, Aug. 2005.

[42] J. C. Synder, H. Bluestein, G. Zhang, and S. J. Frasier, "Attenuation correction and hydrometeor classification of high-resolution, X-band, dual-polarized mobile radar measurements in severe convective storms," *J. Atmos. Ocean. Technol.*, vol. 27, no. 12, pp. 1979–2001, Dec. 2010.

[43] S. Lim, V. Chandrasekar, P. Lee, and A. P. Jayasumana, "Real-time implementation of a network-based attenuation correction in the CASA IP1 testbed," *J. Atmos. Ocean. Technol.*, vol. 28, no. 2, pp. 197–209, Feb. 2011.

[44] L. Lei, G. Zhang, R. J. Doviak, R. Palmer, B. L. Cheong, M. Xue, Q. Cao, and Y. Li, "Multilag correlation estimators for polarimetric radar measurements in the presence of noise," *J. Atmos. Ocean. Technol.*, vol. 29, no. 6, pp. 772–795, Jun. 2012.

[45] F. Fabry, "Meteorological value of ground target measurements by radar," *J. Atmos. Ocean. Technol.*, vol. 21, no. 4, pp. 560–573, Apr. 2004.

[46] B. L. Cheong, R. D. Palmer, C. D. Curtis, T.-Y. Yu, D. S. Zrnić, and D. Forsyth, "Refractivity retrieval using the Phased Array Radar: First results and potential for multi-function operation," *IEEE Trans. Geosci. Remote Sens.*, vol. 46, no. 9, pp. 2527–2537, Sep. 2008.

Boon Leng Cheong received the B.S.E.E., M.S.E.E., and Ph.D. degrees in electrical engineering from the University of Nebraska, Lincoln, NE, USA, in 1999, 2002, and 2005, respectively.

He has been with the University of Oklahoma, Norman, OK, USA, since 2005, as a Post-Doctoral Fellow with the School of Meteorology. In 2009, he joined the Advanced Radar Research Center as a Research Scientist, where he has participated in various projects related to radar meteorology. He is currently an Adjunct Assistant Professor with the School of Electrical and Computer Engineering and an Executive Member of the Board of Directors of the Cooperative Institute for Mesoscale Meteorological Studies. His current research interests include numerical radar simulations, array processing using multiple receivers, and image processing using artificial intelligence.

Redmond Kelley received the bachelor's and master's degrees in electrical engineering from the University of Oklahoma, Norman, OK, USA, in 2007 and 2009, respectively.

He is a Staff Engineer with the Advanced Radar Research Center (ARRC) and one of the technical managers of the ARRC's Radar Innovations Laboratory. He began his research in IF-sampling digital radar receiver technology and focus to radar hardware systems development. He supports most of the ARRC's hardware research projects and specializes in system level design/integration, analog/digital circuit design, and multilayer printed circuit board layout/fabrication/assembly. His current research interests include the design of cost-effective conventional, imaging, and phased array radar technologies.

Robert D. Palmer was born in Fort Benning, GA, USA, on June 3, 1962. He received the Ph.D. degree in electrical engineering from the University of Oklahoma (OU), Norman, OK, USA, in 1989.

He was a JSPS Post-Doctoral Fellow with the Radio Atmospheric Science Center, Kyoto University, Kyoto, Japan, from 1989 to 1991, where his major accomplishments were the development of novel interferometric radar techniques for studies of the lower and middle atmosphere. From 1993 to 2004, he was a Faculty Member with the Department of Electrical Engineering, University of Nebraska, Lincoln, NE, USA. He is currently the Tommy C. Craighead Chair with the School of Meteorology, OU, where he is an Adjunct Professor with the School of Electrical and Computer Engineering. He serves as an Associate Vice President for Research and Director of OU's Interdisciplinary Advanced Radar Research Center, which is the focal point for radar research and educational activities on the Norman campus. His research interests focused on the application of advanced radar signal processing techniques to observations of severe weather, particularly related to phased-array radars and other innovative system designs. He has published widely in the area of radar remote sensing of the atmosphere, with an emphasis on generalized imaging problems, spatial filter design, and clutter mitigation using advanced array/signal processing techniques. His current research interests include wireless communications, remote sensing, and pedagogy.

Prof. Palmer is a member of URSI Commission F, the American Geophysical Union, and the American Meteorological Society. He has been a recipient of several awards for both his teaching and research accomplishments.

Yan Zhang (S'03–M'04) was born in Beijing, China. He received the B.S. and M.S. degrees in electrical engineering from the Beijing Institute of Technology, Beijing, China, in 1998 and 2001, respectively.

He was a Research Assistant with the Environmental Remote Sensing Laboratory, University of Nebraska, Lincoln, NE, USA, from 2001 to 2004. From 2004 to 2007, he was a Research Scientist with Intelligent Automation, Inc., Rockville, MD, USA. He is currently serving as an Associate Professor with the School of Electrical and Computer Engineering, University of Oklahoma, Norman, OK, USA. He has been the Lead with the Intelligent Aerospace Radar Team and an Engineering Lead with the Atmospheric Radar Research Center. He has been focusing on application-oriented research on electromagnetic systems, RF/microwave system for weather radars, and advanced radar engineering from concept to implementations.

Mark Yeary (S'95–M'00–SM'03) received the B.S. (Hons.), M.S., and Ph.D. degrees from Texas A&M University, College Station, TX, USA, in 1992, 1994, and 1999, respectively.

He is currently with the School of Electrical and Computer Engineering, University of Oklahoma (OU), Norman, OK, USA, and with OU's Advanced Radar Research Center, where he is a Full Professor. His current research interests include digital signal processing (DSP) as applied to customized DSP systems, tactical radars, and weather radars, with an emphasis on hardware prototype development. He was with Raytheon, Dallas, TX, USA, as a Faculty Researcher, from 2002 to 2011, which includes target detection and tracking studies. He was with the Lincoln Laboratory, Massachusetts Institute of Technology, Cambridge, MA, USA, in 2012 and 2013, as a Visiting Researcher.

Dr. Yeary is a member of the Tau Beta Pi and Eta Kappa Nu honor societies and is a Licensed Professional Engineer. He was a recipient of the IEEE 2005 Outstanding Young Engineer Award from the Instrumentation and Measurement (I&M) Society for "contributions to radar measurements." He has served as a Technical Committee Member for the IEEE International Instrumentation and Measurement Conference on several occasions and as a Technical Co-Chair for the I2MTC in 2010. He currently serves as an I&M Associate Editor and a member of its Administrative Committee.

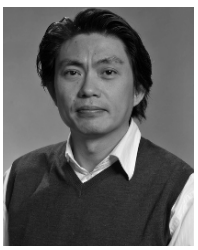

Tian-You Yu received the Ph.D. degree in electrical engineering from the University of Nebraska-Lincoln, Lincoln, NE, USA, in 2000.

He is a Professor with the School of Electrical and Computer Engineering and an Adjunct Associate Professor with the School of Meteorology, University of Oklahoma, Norman, OK, USA. He is an Associate Director with the Advanced Radar Research Center, which is an Interdisciplinary Research Center. He held a post-doctoral position with the National Center for Atmospheric Research, providing a unique cross-disciplinary background of atmospheric research using various sensors. He has many reviewed technical journal and conference papers in the areas of applications of signal processing techniques to radar problems and studies using atmospheric radars. He has a passion for delivering high quality education. He has developed and taught several undergraduate and graduate courses with the University of Oklahoma.

Dr. Yu currently serves as an Associate Editor of the *Journal of Radio Science*.